IBRACON Structures and Materials Journal
Revista IBRACON de Estruturas e Materiais
ISSN 1983-4195 ismj.org

ORIGINAL ARTICLE

Steel failure mode of composite dowel shear connector with rectangular regular cutoff

Modo de falha do aço do conector de cisalhamento com corte regular retangular

Eliane Gomes da Silveira[a]
Rodrigo Barreto Caldas[b]
Lucas Ribeiro dos Santos[b]

[a]Instituto Federal de Educação, Ciência e Tecnologia do Sul de Minas Gerais – IFSULDEMINAS, Departamento de Engenharia Civil, Pouso Alegre, MG, Brasil
[b]Universidade Federal de Minas Gerais – UFMG, Departamento de Estruturas, Belo Horizonte, MG, Brasil

Received 17 October 2022
Revised 17 April 2023
Accepted 22 June 2023
Corrected 27 March 2024

Abstract: In this work, a study was carried out on the steel failure behavior of composite dowel shear connectors with regular rectangular cutoff. The bearing capacity equation related to the steel failure is normally treated in the literature as a function of the thickness, yield strength, geometric repetition and shape coefficient. The connector with regular rectangular cutoff study comprised the deduction of the steel failure equation according to von Mises criterion and the comparison of the results obtained from numerical analysis produced for this work and experimental results from literature. The shape coefficient found in each phase of the study is presented. Furthermore, from the numerical results it was possible to evaluate the stress distribution on the steel dowel and verify the coherence of the mechanical model that considers a straight critical section and a uniformly distributed load due to the concrete pressure on the steel dowel.

Keywords: shear connector, composite dowels, steel failure, mechanical behavior, rectangular regular cutoff.

Resumo: Neste trabalho foi realizado um estudo sobre o comportamento à falha do aço dos conectores de cisalhamento fabricados com recortes regulares retangulares. A equação para a capacidade resistente relacionada à falha do aço da conexão é normalmente tratada na literatura em função da espessura, da resistência ao escoamento da chapa do conector, da repetição geométrica e do fator de forma. O estudo do conector com recorte regular retangular compreendeu a dedução da equação para a falha do aço segundo o critério de von Mises e a comparação dos resultados obtidos com resultados numéricos produzidos para esse trabalho e experimentais provenientes de outros trabalhos. É apresentado o fator de forma encontrado em cada fase do estudo. Além disso, a partir dos resultados numéricos foi possível avaliar a distribuição de tensões sobre o pino de aço do conector e verificar a coerência do modelo mecânico que considera uma seção crítica retilínea e um carregamento uniformemente distribuído devido à pressão do concreto sobre o pino de aço.

Palavras-chave: conector de cisalhamento, conector em chapa, falha do aço, comportamento mecânico, corte regular retangular.

How to cite: E. G. Silveira, R. B. Caldas, and L. R. Santos, "Steel failure mode of composite dowel shear connector with rectangular regular cutoff," *Rev. IBRACON Estrut. Mater.*, vol. 17, no. 3, e17310, 2024, https://doi.org/10.1590/S1983-41952024000300010

1 INTRODUCTION

Initially, steel plated shear connectors were developed for application in bridges, as an alternative that offered greater rigidity and fatigue resistance at the steel-concrete interface in relation to existing connectors, especially stud bolt. The first steel plated connector with holes (Perfobond) was used in 1987 on the Caroni River bridge in Venezuela, proposed by the German company *Leonhardt, Andrä und Partner* [1]. Several other steel plated shear connectors were proposed after

Corresponding author: Eliane Gomes da Silveira. E-mail: eliane.silveira@ifsuldeminas.edu.br
Financial support: None.
Conflict of interest: Nothing to declare.
Data Availability: The data that support the findings of this study are available from the corresponding author, [EGS], upon reasonable request.
This document has an erratum: https://doi.org/10.1590/S1983-41952024000300011

Perfobond, with cuts in different geometries, including open and with continuous regular cutoff [1]–[7]. In Brazil, in 2007, the Crestbond steel plated connector was presented, whose plate is cut in a continuous trapezoidal symmetrical way, which provides adequate strength to longitudinal shear and prevents the uplift effect when applied to composite beams [8]–[11].

Following the same study trend, in 2013 a research project with beams was started named PreCoBeam [12], [13] whose objective was to develop continuous steel plated connectors for road bridges composite beams, obtained from the regular cutoff in the web of I profiles. Among the main cutoff geometries studied are clothoidal, puzzle and fin. The research program resulted in the development of the German technical approval Z-26.4-56 [14], which presents design criteria for puzzle and clothoidal steel plated connectors. The document predicts three possible failure modes for steel plated connectors: steel failure, concrete shear and pry-out. The design equations consider continuous connectors and present coefficients dependent on the cutting geometry of the connector, through shape coefficient. The equation for steel failure is presented in Z-26.4-56 [14] as a function of pitch, plate thickness, steel connector yield strength and a coefficient related to the shape of the cutoff.

Most of the research carried out with steel plated connectors found in the literature refers to the application in steel-concrete composite beams and slabs [3], [4], [10]–[13], [15]–[21]. Recently, researchers from the Federal University of Minas Gerais carried out studies with the application of steel plated connectors in concrete-filled steel tubular columns (CFST) [2], [22]–[29]. In this type of application, the connector can perform the function of a load transfer element and act as an end plate for connecting beams to the column [2].

The inherent CFST behavior allows the efficient application of composite dowels connectors, even with a single connector installed in the beam-column connection region. The effects of stress concentration are overcome by the global concrete confinement effect by the tube and by the local confinement in the loaded region immediately below the connector. Such effects contribute for the concrete to present greater resistance capacity and ductility, making the initial cracking process more difficult. Furthermore, when the concrete is prevented from expanding radially by the tube, the contact pressure is increased and the materials engagement between the connector and the concrete is increased, contributing to the stresses transmission. It is noteworthy that in practice it is usual to install stirrups in the concrete core, which also contribute to the concrete confinement and to the stresses redistribution in the concrete dowels, in addition to limiting steel dowels deformations.

For this type of application, the experimental results with composite dowels connectors indicate a rigid and ductile behavior for the Crestbond and regular rectangular geometries [2], [8]–[11], [22], [26], [29], which avoids fatigue fail at ultimate limit state. So far, there are no published studies that indicate a significant influence of residual stress in the welding process of these connectors and that affect the fatigue life.

The first studies with steel plated shear connectors indicated the shearing of the concrete in the openings as the predominant failure mode. As new geometries were studied, the size of concrete-filled openings became equal to or larger than steel dowels, leading to new failure modes of the composite connection, such as connector steel failure. With this, the steel plated shear connectors started to be identified as composite dowels, having concrete and steel dowels [2]. The load transfer in the composite dowels is essentially done by the interaction between the steel and concrete dowels, by shear. For small relative slips between the steel profile and the concrete, the lower region of the connector is subjected to a resultant force from the shear stresses (F_v). A resultant of the same magnitude and opposite direction also appears in the composite element, performing the balance of forces. In steel and concrete dowels, there is a mutual interaction through contact stresses at the interface, and thus the efforts between the dowels are transferred [2]. The contact interface between steel and concrete dowels varies depending on the geometry of the connector. In connectors with the same steel dowel and the concrete dowel geometry such as Crestbond and puzzle, the concrete dowel is bounded by the steel dowel, and the entire height of the steel dowel is in contact with the concrete dowel. In connectors with different geometry for the concrete and steel dowel, such as clothoidal, the height of the concrete dowel that interacts with the steel dowel is smaller [30].

In this article, the equation for steel dowel failure is deduced according to von Mises criterion, for a uniformly distributed loading as suggested by Feldman et al. [31], considering the regular rectangular cutoff. The results obtained with the equation are then compared with experimental and numerical values of connectors with regular rectangular cutoff applied in CFST. The equation was also used in an analytical study where geometric and material parameters of the connectors were varied. Finally, an analysis of the stress distribution in the steel dowels of the connector is presented.

2 STEEL DOWEL MECHANICAL MODEL ACCORDING TO VON MISES CRITERIA

According to Feldman et al. [31], there is a critical section in the steel dowel where failure will occur or start due to the requests that occur in the transmission of shear forces between the steel and concrete components of the composite structure. Also, according to the author, the critical section height that will lead to steel dowel failure can be calculated in a simplified way, considering the concrete uniform loading on the steel dowel in all its height, except for the radius of

the top rounded part of the steel dowel. Fig. 1a shows the geometric parameters also considered by Feldman et al. [31] adapted to the composite dowel with regular rectangular cutoff.

Feldman et al. [31] defines that the connector strength for steel failure (P_{pl}) corresponds to the smallest load value that will lead to the maximum von Mises stress in a given cross section of the steel dowel. This section will have a certain width (b_{crit}) and distance from the connector base (h_{crit}) depending on its position on the steel dowel.

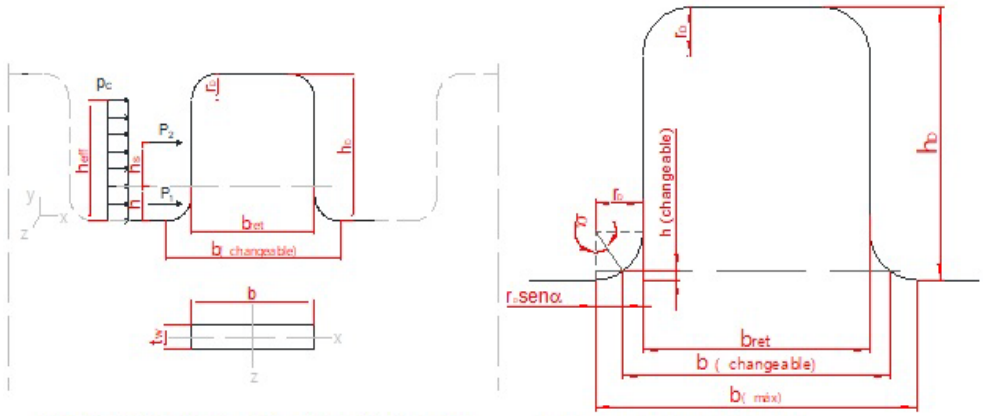

(a) Variables for calculating the critical section (b) Detail of the steel dowel

Fig. 1 - Variables for calculating the critical height according to Feldman et al. [31]

According to Feldman et al. [31] and Kopp et al. [3], the critical width (b_{crit}) and the critical height (h_{crit}) of the section in the steel dowel are defined as a function of the maximum von Mises stress produced by the resultant of the distributed loading p_c (P_{pl}), which causes shear and normal stresses due to the shear force and bending moment in the critical section, defined by Equation 1.

$$P_{pl} = \left(1 + \frac{h_{crit}}{h_{eff} - h_{crit}}\right)\left(\frac{b_{crit}}{\sqrt{16h_{s,crit}^2 + 3b_{crit}^2}}\right) b_{crit} t_w f_y \tag{1}$$

The steel dowel yielding occurs from the effects composition of the shear force and the bending moment, resulting from the force transferred from the infill concrete (concrete dowel) to the steel dowel.

There are some alternatives to determine the critical section height (h_{crit}) in the steel dowel of the connector: it is possible to carry out an iterative process of searching for the maximum von Mises stress value in the section, with the variation of the distance value of the section (h) for a distributed unit load; another possibility is the variation of the height section value (h_{crit}), applying to Equation 1, thus determining the smallest P_{pl} value within the effective height (h_{eff}). Another more efficient process consists in determining the minimum point of the P_{pl} function as a function of the distance or height section (h). Although more objective, this method results in an extensive equation, which will be presented below.

In Fig. 1a the variables h, b and h_s receive the subindex *"crit"* in Equation 1 when is determined the smallest force P_{pl} that leads to the maximum von Mises stress in the steel dowel section and consequently to failure. As this value is determined by an iterative process, the subindex will be suppressed during the deduction of the equation, until the form presented in Equation 1 is found.

The steel dowel in the shear connector with regular rectangular cutoff has rounded corners, which can mean a larger dowel width (b) if the section distance (h) is smaller than the curvature radius (lower rounded corner on steel dowel). Thus, it will be considered that the steel dowel width value is variable as a function of the height section, as shown in Fig. 1b.

The section distance h defines the angle α (Fig. 1c), thus defining the dowel width b (Equation 2 and 3).

$$\boldsymbol{r_D \cos\alpha = r_D - h} \qquad \Rightarrow \qquad \boldsymbol{\cos\alpha = \frac{r_D - h}{r_D}} \qquad \therefore \qquad \boldsymbol{\alpha = arccos\left(\frac{r_D - h}{r_D}\right)} \tag{2}$$

$$\boldsymbol{b = 2(r_D - r_D sin\,\alpha) + b_{ret} \quad \Rightarrow \quad b = 2r_D(1 - sin\,\alpha) + b_{ret} \quad \Rightarrow \quad b = 2r_D\left[1 - sin\left(arccos\left(\frac{r_D - h}{r_D}\right)\right)\right] + b_{ret}} \tag{3}$$

The steel dowel width (b) then varies as a function of the section height position (h):

$$\begin{cases} \boldsymbol{h < r_D \rightarrow \; b = 2r_D\left[1 - sin\left(arccos\left(\frac{r_D - h}{r_D}\right)\right)\right] + b_{ret};} \\ \boldsymbol{h \geq r_D \; \rightarrow \; b = b_{ret}} \end{cases} \tag{4}$$

Using the von Mises criterion, it is possible to deduce the equation for the connector steel failure strength (P_{pl}), for that, it is necessary to establish what will be the resultant force that will produce the stress components due to the shear force and bending moment in the critical section. From Fig. 1 it is observed that the force P_1, acting below the established section, does not generate tensions in the analyzed section (which are of interest for the development of the equation). On the other hand, the resultant force P_2, above the section, will request the section causing normal and shear stresses due to the bending moment and shear force.

The force P_2 corresponds only to the resultant portion of the distributed loading p_c that produces the bending moment and the shear force in the section, which may be the critical section along the height of the steel dowel. To determine the distributed loading resultant of the concrete on the steel dowel that produces plasticization or failure of the same, it is necessary to make the following conversion:

$$P_{pl} = p_c \cdot h_{eff} \qquad \therefore \qquad p_c = \frac{P_{pl}}{h_{eff}} \tag{5}$$

From Equation 5, the force P_2 can be defined as follows:

$$P_2 = 2h_s \cdot \frac{P_{pl}}{h_{eff}} \tag{6}$$

And the force P_2, which produces the stress components due to the bending moment and the shear force, can be defined as:

$$P_2 = \left(\frac{b}{\sqrt{16h_s^2 + 3b^2}}\right) f_y t_w b \tag{7}$$

where b is defined by Equation 4, as a function of the section height.

Substituting Equation 6 in Equation 7, we have:

$$\begin{gathered} 2h_s \cdot \frac{P_{pl}}{h_{eff}} = \left(\frac{b}{\sqrt{16h_s^2 + 3b^2}}\right) f_y t_w b \quad \Rightarrow \quad P_{pl} = \left(\frac{h_{eff}}{2h_s}\right)\left(\frac{b}{\sqrt{16h_s^2 + 3b^2}}\right) f_y t_w b \quad \Rightarrow \\ \Rightarrow \quad P_{pl} = \left(\frac{h_{eff}}{h_{eff} - h}\right)\left(\frac{b}{\sqrt{16h_s^2 + 3b^2}}\right) f_y t_w b \quad \Rightarrow \quad P_{pl} = \left[\frac{(h_{eff} - h) + h}{h_{eff} - h}\right]\left(\frac{b}{\sqrt{16h_s^2 + 3b^2}}\right) f_y t_w b \quad \Rightarrow \\ \Rightarrow \quad P_{pl} = \left(1 + \frac{h}{h_{eff} - h}\right)\left(\frac{b}{\sqrt{16h_s^2 + 3b^2}}\right) f_y t_w b \end{gathered} \tag{8}$$

Equation 8 has the same form as the equation proposed by Feldman et al. [31] (saving the differences regarding the symbology used), provided that the critical height and width at the dowel are considered to determine the connector steel failure strength. In order to avoid the calculation of the critical height through iterative process with the variation of the

height value h in Equation 8, the first derivative of Equation 8 can be determined as a function of height h and set it to zero. The value of h that conducts Equation 9 to zero represents the h_{crit}. The h_{crit} values and the corresponding steel dowel width (b_{crit}) can be used in Equation 8, and give Equation 8 the same form as the equation proposed by Feldman et al. [31]. In this way, the lowest value of P_{pl} that leads to the connector steel failure with regular rectangular geometry is determined.

$$\frac{dP_{pl}}{dh} = \frac{f_y t_w \left(b_{ret} + 2r_D \left(1 - \sqrt{1 - \frac{(r_D - h)^2}{r_D^2}} \right) \right)^2 \left(\frac{1}{h_{eff} - h} + \frac{h}{(h_{eff} - h)^2} \right)}{\sqrt{3 \left(b_{ret} + 2r_D \left(1 - \sqrt{1 - \frac{(r_D - h)^2}{r^2}} \right) \right)^2 + 4(h_{eff} - h)^2}} - \frac{4 f_y t_w \left(b_{ret} + 2r_D \left(1 - \sqrt{1 - \frac{(r_D - h)^2}{r_D^2}} \right) \right) (r_D - h) \left(1 + \frac{h}{h_{eff} - h} \right)}{r_D \sqrt{3 \left(b_{ret} + 2r_D \left(1 - \sqrt{1 - \frac{(r_D - h)^2}{r_D}} \right) \right)^2 + 4(h_{eff} - h)^2} \cdot \sqrt{1 - \frac{(r_D - h)^2}{r_D^2}}} - \frac{f_y t_w \left(b_{ret} + 2r_D \left(1 - \sqrt{1 - \frac{(r_D - h)^2}{r_D}} \right) \right)^2 \left(-8(h_{eff} - h) - \frac{12 \left(b_{ret} + 2r_D \left(1 - \sqrt{1 - \frac{(r_D - h)^2}{r_D^2}} \right) \right) (r_D - h)}{r_D \sqrt{1 - \frac{(r_D - h)^2}{r_D}}} \right) \left(1 + \frac{h}{h_{eff} - h} \right)}{2 \left(3 \left(b_{ret} + 2r_D \left(1 - \sqrt{1 - \frac{(r_D - h)^2}{r_D^2}} \right) \right)^2 + 4(h_{eff} - h)^2 \right)^{3/2}} = 0 \quad (9)$$

2.1. Comparison of the connector steel failure model with experimental results

The experimental results presented by Caldas et al. [29] of composite dowels with regular rectangular cutoff applied to concrete-filled steel tubular columns (CFST) were used to verify the results produced by Equation 9 and Equation 8 (with Equation 9 the h_{crit} value was obtained and used in Equation 8 to determine the steel failure strength). The reference connector consists of a 12.5 mm thick plate, cut with three steel dowels 70 mm high and 60 mm wide (Fig. 2). The connector was applied to CFST with circular and rectangular tubes, totaling 5 experimental series.

In Tab. 1 are indicated the maximum load achieved in test for each specimen ($P_{u,Exp}$), the maximum load per connector ($q_{cn,Exp}$), the maximum load in test per steel dowel ($P_{max,1}$), maximum characteristic capacity per dowel, defined by the lowest maximum test load per dowel reduced by 10% (P_{Rk}), the maximum design capacity per dowel, calculated according to Equation 10 (Kozuch e Lorenc [15] and EN 1994-1-1 [32]) and the experimental shape coefficient, calculated for the smallest experimental value $P_{max,1}$ according to Equation 11 (Kozuch e Lorenc [15]).

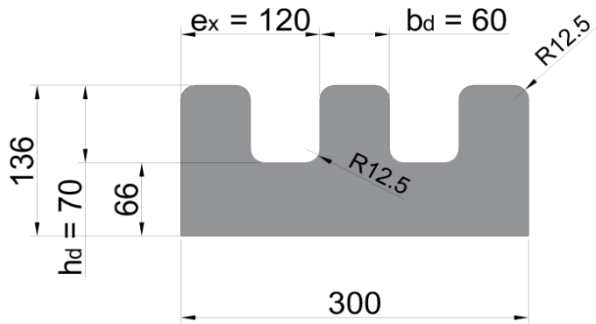

Fig. 2 - Composite dowel shear connector with regular rectangular cutoff. Measures in millimeters.

$$P_{Rd} = \frac{f_y}{f_{yt}} \cdot \frac{P_{Rk}}{\gamma_v} \tag{10}$$

$$A_{ULT,test} = \frac{P_{max,1}}{e_x \cdot t_w \cdot f_y} \tag{11}$$

where e_x is the dowel spacing.

Tab. 1 – Shape coefficient calculated according to experimental data from Caldas et al. [29].

Specimen	$P_{u,Exp}$ (kN)	$q_{cn,Exp}$ (kN)	$P_{max,1}$ (kN)	P_{Rk} (kN)	P_{Rd} (kN)*	$A_{ULT,test}$
D1	**1504.31**	**752.15**	**250.72**	**225.65**	**180.00**	**0.429**
D2	**1516.83**	**758.42**	**252.81**			
E1	**-**	**-**	**-**	**303.00**	**241.71**	**0.576**
E2	**2020.02**	**1010.01**	**336.67**			
R1	**2268.69**	**1134.35**	**378.12**	**337.15**	**268.95**	**0.640**
R2	**2247.67**	**1123.83**	**374.61**			
X1	**1263.84**	**631.92**	**210.64**	**168.56**	**134.46**	**0.320**
X2	**1123.73**	**561.87**	**187.29**			
Y1	**1275.98**	**637.99**	**212.66**	**191.39**	**152.68**	**0.363**
Y2	**1276.71**	**638.35**	**212.79**			

* steel of the connector USI CIVIL 350 and γ_v = 1.25.

The variation between the experimental results presented in Tab. 2 is essentially due to the concrete confinement by tube in the CFST. This fact was also confirmed by Cardoso et al. [2] and Cardoso [22] in the application of Crestbond connectors in CFST under similar conditions. In the first three series D, E and R, circular profiles were used and, in the last two, X and Y, rectangular profiles.

By varying the section distance (h) every 0.5 mm in Equation 8, it is possible to obtain the steel failure strength curve for the reference connector, as shown in Fig. 3. Simply, from Equation 9 the highlighted minimum point is obtained, for which we have the critical section height h_{crit} (5.93 mm) and the connector steel failure strength P_{pl} equal to 146.14 kN.

The connector steel failure strength P_{pl} calculated from the von Mises criterion (Equation 8) leads to a conservative value of 146.14 kN, about 13% below the lowest resistance value found experimentally for the same connector geometry applied to X series (Tab. 1). For this connector strength value (146.14 kN), the connector shape coefficient is equal to 0.250, considering that the connector steel plate has a thickness (t_w) of 12.5 mm, steel yield strength (f_y) of 390 MPa and pitch or geometric repetition (e_x) equal to 120 mm. On the other hand, the average experimental shape coefficient considering the 5 series (identified by Kozuch e Lorenc [15] as $A_{ULT,test}$) is equal to 0.466.

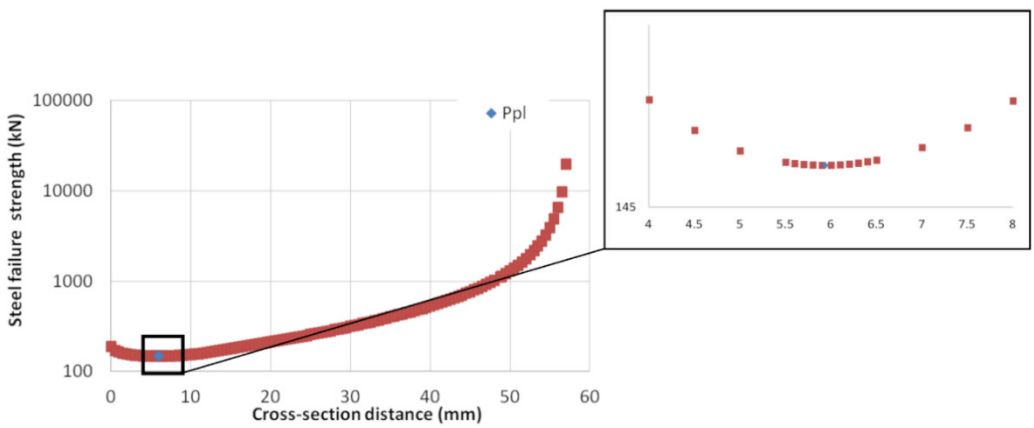

Fig. 3 - Connector steel failure strength curve, according to von Mises criterion, varying as a function of the section height considered in the steel dowel.

2.2. Comparison of the connector steel failure model with numerical results

Two series of numerical simulations were carried out to study the shear connector with regular rectangular cutoff. The details of model calibration and validation are properly described in Caldas et al. [29], and were developed according to Cardoso et al. [2] and Santos et al. [23]-[25]. The first series corresponds to the numerical models developed by Caldas et al. [29] to represent the experimental results of shear connectors with regular rectangular cutoff applied in CFST. For this numerical results series, the shape coefficient was calculated according to Lorenc [17], which superimposes force-slip curves obtained from the numerical simulation considering the perfect elasto-plastic steel behavior of the connector with another in which the hardening is considered and an unloading branch for the steel connector behavior. Lorenc [17] considers that the characteristic resistance of the connector is equal to the last convergent point between the relative force-slip curves for the aforementioned simulations.

The second numerical simulations series consisted of a parametric study with a square CFST with a side of 250 mm, for which the tube thickness, the connector plate thickness, the steel yield strength of the connector and the tube, the steel dowels width and height, the connector base height inside the tube, the number of steel dowels and the concrete compressive strength were varied. The results of this numerical study were compared with the analytical ones obtained through Equation 8.

The specimens were simulated using the finite analysis software Abaqus 6.14, consisting of a steel tube, composite dowel connector, concrete core and steel reinforcement. Considering the double symmetry, a quarter of the CFST model was modeled, with constraints being assigned to the planes of symmetry. The steel tube, concrete core and connector were modeled with C3D8 eight-node brick elements and the reinforcement with B31 two-node beam elements. An 8 mm mesh was applied to the connector and in the region near the shear connection, in other regions the mesh gradually increased in size as it distance from the connector, reaching 50 mm.

The interactions of the contact interfaces between connector-concrete and tube-concrete, a hard contact type was adopted in the normal direction and in the tangential direction the penalty frictional formulation type with coefficient of friction $\mu = 0.5$ for connector-concrete and $\mu = 0.07$ for tube-concrete. Tie constraint was applied in the weld region between connector and tube and embedded constraint to simulate concrete-reinforcement interaction.

A displacement-controlled load was applied to a reference point centered on the core, located 30 mm above the model, displaced in an axial direction against the model and coupled to the steel tube top surface by coupling constraint. For the iterative analysis, the quasi-static Dynamic Implicit method was used, which led to results with better convergence.

To simulate the concrete nonlinear behavior, the model available in the software concrete damaged plasticity was used, with the relationship adopted for the compressive behavior of concrete according to EN 1992-1-1:2004 and the extension of the curve according to the study of Pavlovic et al. [35]. The tension behavior of the uncracked concrete followed the Bézier cubic function calibrated according to Kim and Nguyen [36]. The functions that define the concrete behavior curves and other parameters can be found in Cardoso et al. [2] and Caldas et al. [29].

The steel behavior for the reinforcement was considered as perfect elastoplastic. For the steel connector behavior, the curve presented by Cardoso et al. [2] which considers hardening the steel and a cut-off stage with softening branch, an approach also used by Lorenc et al. [18] to simulate crack propagation.

2.2.1. Numerical reproduction of experimental specimens

The Tab. 2 presents the calculated shape coefficient for each numerical model corresponding to the experimental series [29]. The force values P_{num} presented were obtained according to Lorenc [17], which considers the connector strength corresponding to the last converging point between the force-slip numerical curves, considering in a numerical analysis the elasto-plastic steel behavior of the connector (Curve b) and the steel hardening (Curve a) in a second analysis. Fig. 4 exemplifies obtaining the force P_{num} for the R* numerical model. The average shape coefficient for the numerically simulated experimental series is equal to 0.311.

Tab. 2 – Shape coefficient obtained from numerical modeling of experimental results.

Series	P_{num} (kN)	q_{num} (kN)	$P_{max,1}$ (kN)	$A_{ULT,num}$	$P_{num}/P_{u,Exp}$	$A_{ULT,num}/A_{ULT,test}$
D*	1081.16	540.58	180.19	0.308	0.72	0.72
E*	1209.18	604.59	201.53	0.344	0.60	0.60
R*	1157.34	578.67	192.89	0.330	0.51	0.51
X*	1018.66	509.33	169.78	0.290	0.91	0.91
Y*	985.8	492.90	164.30	0.281	0.77	0.77

Series are identified followed by * to indicate that they are based on experimental results.

It is important to highlight that the $A_{ULT,test}$ values are based on resistance average values obtained experimentally, while the values of $A_{ULT,num}$ are based on the methodology of Lorenc [17], in terms of characteristic resistance. With this, it is expected that the ratio values $A_{ULT,num}/A_{ULT,test}$ are always less than 1.00.

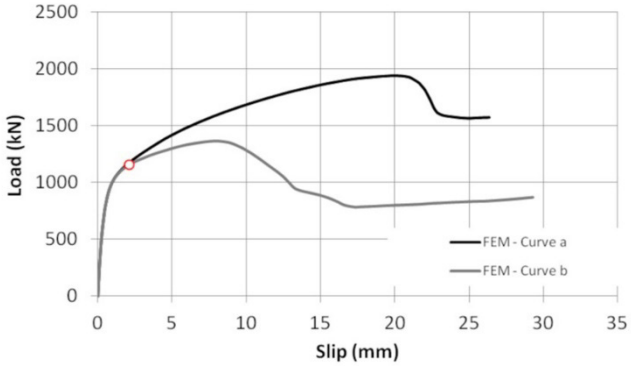

Fig. 4 – Shape coefficient determination for shear connector with regular rectangular cutoff (R serie).

For the series presented in this work, the average ratio $A_{ULT,num}/A_{ULT,test}$ is equal to 0.7. The models analyzed experimentally and numerically by Kozuch e Lorenc [15] also showed an $A_{ULT,num}/A_{ULT,test}$ ratio around 0.7.

2.2.2. Parametric study

The Tab. 3 shows the main parameters varied in this phase of studies. The A model was adopted as a reference for the variation of parameters. Tab. 4 shows the numerical results for the models with the respective shape coefficient (calculated according to Equation 11). The average shape coefficient value for the square profiles series of 250 mm with b_{ret}/h_D = 0.86 is equal to 0.280.

Tab. 3 – Numerical models main variables of the parametric study.

Model	B (mm)	t (mm)	b_{ret} (mm)	h_D (mm)	t_w (mm)	e_x (mm)	c_{bc} (mm)	n	n_c	f_y (MPa)	f_c (MPa)	f_{yt} (MPa)
A	250	**4.00**	60	70	12.5	120	20	3	2	350	40	350
B	250	**1.50**	60	70	12.5	120	20	3	2	350	40	350
C	250	**8.00**	60	70	12.5	120	20	3	2	350	40	350
D	250	4.00	60	70	**8.0**	120	20	3	2	350	40	350
E	250	4.00	60	70	**16.0**	120	20	3	2	350	40	350
F	250	4.00	60	70	12.5	120	20	3	2	350	40	**250**
G	250	4.00	60	70	12.5	120	20	3	2	350	40	**450**
H	250	4.00	60	70	12.5	120	20	3	2	**250**	40	350
I	250	4.00	60	70	12.5	120	20	3	2	**450**	40	350
J	250	4.00	60	70	12.5	120	20	3	2	350	**30**	350
K	250	4.00	60	70	12.5	120	20	3	2	350	**50**	350
L	250	4.00	60	70	12.5	120	20	**2**	2	350	40	350
M	250	4.00	60	70	12.5	120	20	**1**	2	350	40	350
N	250	4.00	60	70	12.5	120	20	**4**	2	350	40	350
O	250	4.00	**50**	**65**	12.5	100	20	3	2	350	40	350
P	250	4.00	**80**	**80**	12.5	160	20	3	2	350	40	350
Q	250	4.00	60	70	12.5	120	**10**	3	2	350	40	350
R	250	4.00	60	70	12.5	120	**30**	3	2	350	40	350

Fig. 5 relates the numerical results to those obtained with Equation 8 for the same connector geometry. It is observed that the equation is essentially conservative in relation to the numerical results. When the changed parameters are the thickness and steel yield strength of the tube, there is no change in the predicted bearing capacity, as well as when the parameters of concrete compressive strength and the connector base height inside the tube are varied. The same limitations regarding these parameters are observable in the steel failure strength equation in document Z-26.4-56 [14], given that the equation was obtained from the same formulation.

Tab. 4 – Numerical results of the parametric study and corresponding shape coefficients.

Model	P_{num} (kN)	q_{num} (kN)	$P_{max,1}$ (kN)	$A_{ULT,num}$
A	891.28	445.64	148.55	0.283
B	750.95	375.47	125.16	0.238
C	988.84	494.42	164.81	0.314
D	672.87	336.43	112.14	0.334
E	1002.25	501.12	167.04	0.249
F	879.67	439.83	146.61	0.279
G	895.27	447.64	149.21	0.284
H	735.65	367.82	122.61	0.327
I	973.32	486.66	162.22	0.240
J	793.87	396.93	132.31	0.252
K	949.82	474.91	158.30	0.302
L	625.12	312.56	156.28	0.298
M	231.98	115.99	115.99	0.221
N	1258.30	629.15	157.29	0.300
O	699.08	349.54	116.51	0.266
P	1198.98	599.49	199.83	0.285
Q	813.81	406.90	135.63	0.258
R	961.28	480.64	160.21	0.305

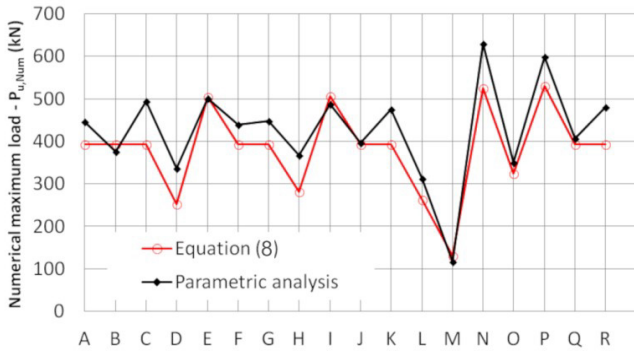

Fig. 5 – Results of the parametric study compared to obtained with Equation 8.

2.3. Analytical study from steel failure equation according to von Mises criterion

In the analytical study, Equation 8 was applied to a series of shear connectors with regular rectangular cutoff with different steel dowel width/height ratios (b_{rel}/h_D) and consequently of the pitch (e_x).

Six series of connectors with b_{rel}/h_D ratios ranging from 0.4 to 1.0 (except for the first series, which included the ratio 0.3) were created. All 6 series were simulated using connectors with plate thicknesses of 12.5 mm and 8.0 mm, and with the connector steel strength of 250 MPa and 350 MPa, usual values used in civil construction for steel tensile strength and plate thickness. The identification of each specimen of the series and the respective geometry are found in Tab. 5.

Tab. 5 – Connector series with geometry variation in steel dowel ratio b_{ret}/h_D for parametric study.

Connector	b_{ret} (mm)	h_D (mm)	$\frac{b_{ret}}{h_D}$	e_x (mm)	r_D (mm)	Connector	b_{ret} (mm)	h_D (mm)	$\frac{b_{ret}}{h_D}$	e_x (mm)	r_D (mm)
CR50-170	50	170	0.3	100	12.5	CR80-200	80	200	0.4	160	12.5
CR50-125	50	125	0.4	100	12.5	CR80-160	80	160	0.5	160	12.5
CR50-100	50	100	0.5	100	12.5	CR80-135	80	135	0.6	160	12.5
CR50-85	50	85	0.6	100	12.5	CR80-115	80	115	0.7	160	12.5
CR50-70	50	70	0.7	100	12.5	CR80-100	80	100	0.8	160	12.5
CR50-65	50	65	0.8	100	12.5	CR80-90	80	90	0.9	160	12.5
CR50-55	50	55	0.9	100	12.5	CR80-80	80	80	1	160	12.5
CR50-50	50	50	1	100	12.5						
CR60-150	60	150	0.4	120	12.5	CR90-225	90	225	0.4	180	12.5
CR60-120	60	120	0.5	120	12.5	CR90-180	90	180	0.5	180	12.5
CR60-100	60	100	0.6	120	12.5	CR90-150	90	150	0.6	180	12.5
CR60-85	60	85	0.7	120	12.5	CR90-130	90	130	0.7	180	12.5
CR60-75	60	75	0.8	120	12.5	CR90-115	90	115	0.8	180	12.5
CR60-70	60	70	0.9	120	12.5	CR90-100	90	100	0.9	180	12.5
CR60-60	60	60	1	120	12.5	CR90-90	90	90	1	180	12.5
CR70-175	70	175	0.4	140	12.5	CR100-250	100	250	0.4	200	12.5
CR70-140	70	140	0.5	140	12.5	CR100-200	100	200	0.5	200	12.5
CR70-120	70	120	0.6	140	12.5	CR100-170	100	170	0.6	200	12.5
CR70-100	70	100	0.7	140	12.5	CR100-145	100	145	0.7	200	12.5
CR70-90	70	90	0.8	140	12.5	CR100-125	100	125	0.8	200	12.5
CR70-80	70	80	0.9	140	12.5	CR100-115	100	115	0.9	200	12.5
CR70-70	70	70	1	140	12.5	CR100-100	100	100	1	200	12.5

Fig. 6 presents the steel failure strength values (P_{pl}) according to Equation 8 as a function of the steel dowel width/height ratio in the shear connectors with regular rectangular cutoff for the six proposed series.

Comparing the results of the steel failure strength equation from the von Mises criterion with the equation suggested by the German technical approval (Z 26.4-56:2018 [14]) it is noted that this is conservative for the CR50, CR60, CR70 and CR80 series in the geometric ratio equal to 1.0, and 0.9 only for the CR50, regardless of the steel yield strength and plate thickness adopted. This fact is exemplified in Fig. 7 for connectors with steel yield strength equal to 350 MPa and plate thickness equal to 12.5 mm, but the same occurs for all other connectors tested (with steel yield strength equal to 250 MPa and plate thickness equal to 8 mm). It is important to note that the steel failure equation proposed by document Z-26.4-56 [14] does not consider the steel dowel height variation in the strength calculation, causing it to remain constant for a series with the same steel dowel width (and consequently the same geometric repetition e_x).

Fig. 8 shows the steel failure strength evolution calculated according to the von Mises criterion (Equation 8) for the series indicated in Tab. 5. For each series, the thickness of the connector and the steel yield strength were varied. In all series, connectors with greater height in relation to width showed lower steel failure strength when compared to connectors with a square shape for the dowel (same measure for height and width of the dowel). This is explained by considering the effects of bending moment and shear force in the equation that determines the critical section. As greater is the steel dowel height, greater is the bending effect on the critical section that would lead to steel failure. Therefore, as greater is the steel dowel width or squarer it is, greater is the steel failure strength.

The average shape coefficient is shown in Tab. 6 in relation to b_{ret}/h_D ratio considered in the analytical study with Equation 8. To simplify comparison with other connector geometries, in Fig. 9 the form factor is related to the e_x/h_D ratio, since in other geometries it is simpler to find values of geometric repetition (e_x).

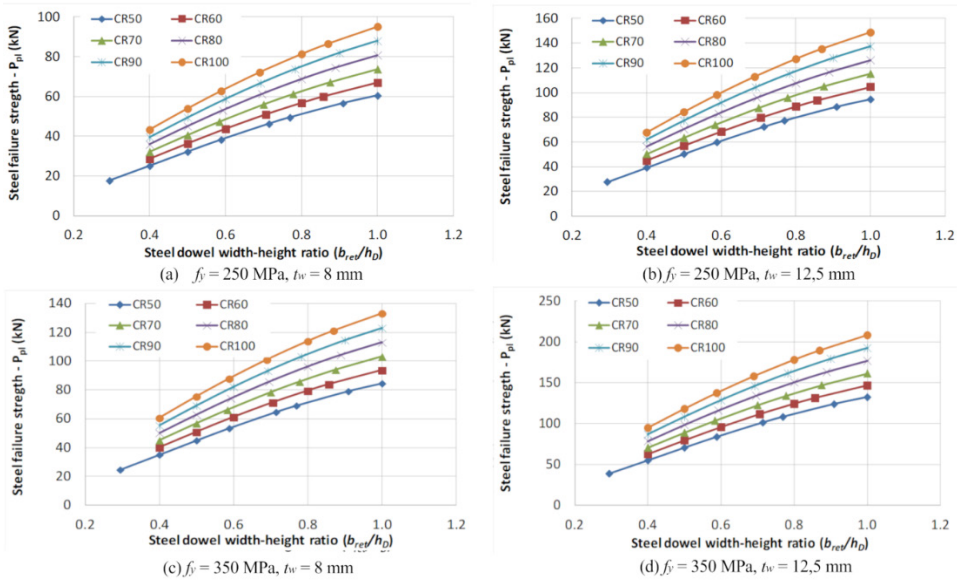

Fig. 6 – Connector steel failure strength as a function of b_{ret}/h_D ratio, steel yield strength (f_y) and plate thickness (t_w).

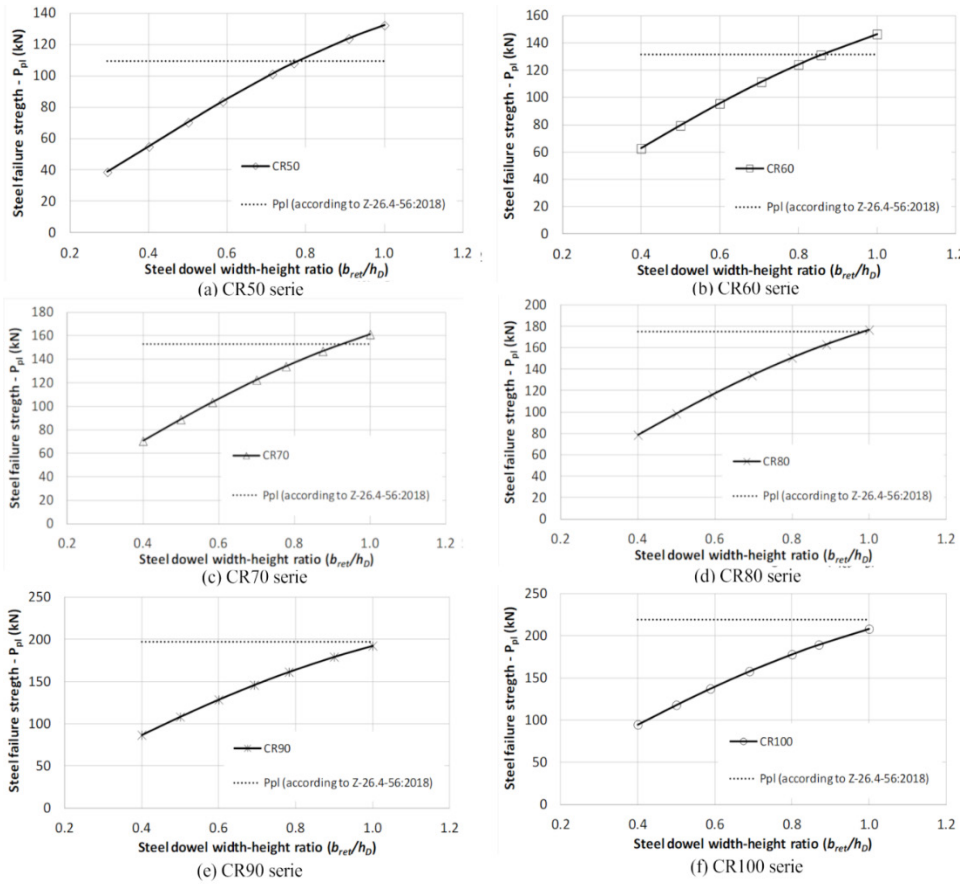

Fig. 7 – Connector steel failure strength as a function of b_{ret}/h_D ratio with f_y = 350 MPa, plate thickness of 12,5 mm, results according to *Equation 8*.

The lines indicated in the graphs correspond to the steel failure strength calculated according to Z 26.4-56 [14].

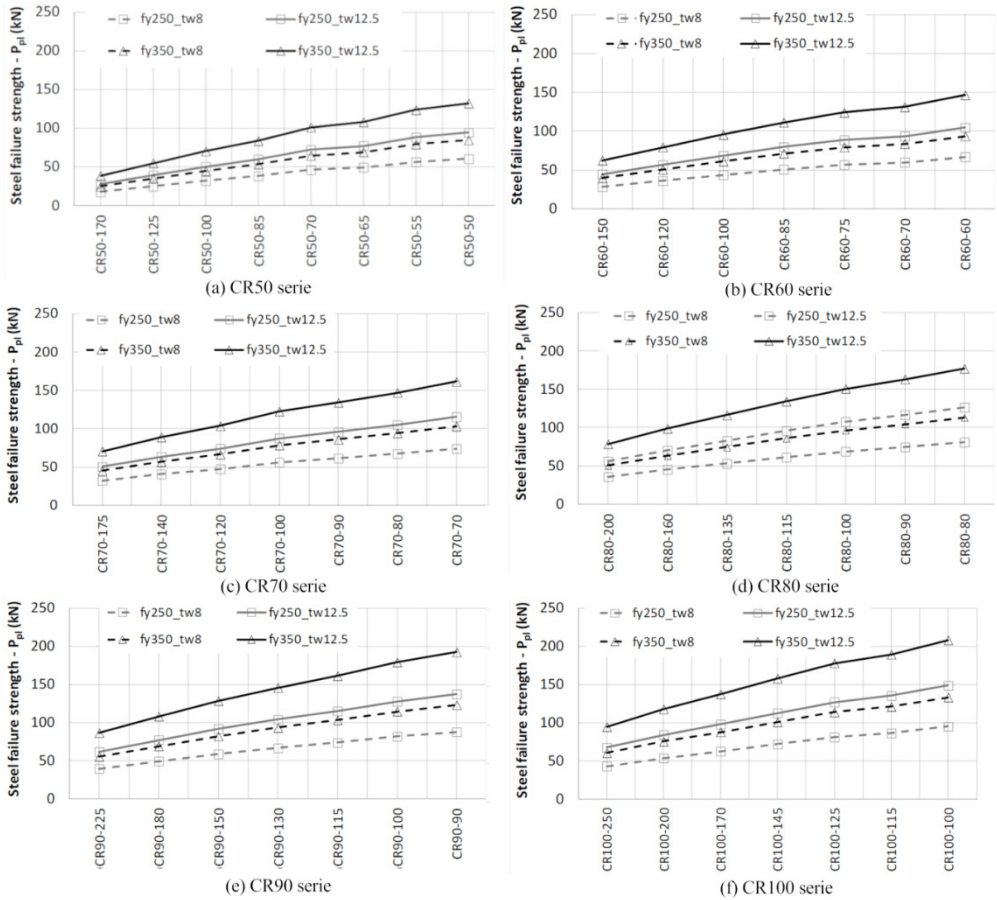

Fig. 8 – Connector steel failure strength according to von Mises criterion, comparing plate thickness and steel yield strength.

Tab. 6 – Average shape coefficient calculated as a function of b_{ret}/h_D ratio according to analytical study.

b_{ret}/h_D	A_{ULT}
0.4	0.115
0.5	0.145
0.6	0.171
0.7	0.200
0.8	0.221
0.9	0.242
1.0	0.263

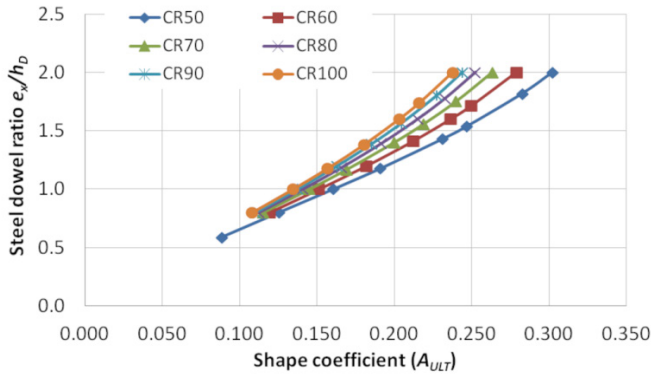

Fig. 9 – Connector shape coefficient as a function of e_x/h_D ratio.

3 STUDY OF STRESS DISTRIBUTION FROM NUMERICAL ANALYSIS

Kozuch and Lorenc [15] argue that the steel dowel behavior model presented by Feldman et al. [31] does not fully represent the steel-concrete interaction in the composite connection, especially for the analysis of the steel failure strength. According to the analysis model proposed by Feldman et al. [31] the failure in the steel dowel occurs following a horizontal plane that represents the critical section, but Kozuch and Lorenc [15], Lechner [16], Rowinski [33] and Kożuch and Rowiński [34] demonstrate in their works through experimental and numerical studies that failure in steel dowel does not occur in a horizontal plane. Furthermore, for Kozuch and Lorenc [15] the uniformly distributed loading along the steel dowel height is a simplification that does not correspond to the real situation, in the same way as the rectangular distribution of normal and shear stresses in the critical section (Fig. 1). For this reason, from the numerical simulation of the experimental results, Kozuch and Lorenc [15] present a distribution of normal and shear stresses as a function of the concrete pressure and friction on the steel dowel along its height, demonstrating that the loading applied on the dowel differs considerably from the simplification adopted by Feldman et al. [31].

Kozuch and Lorenc [15] also argue that for the clothoidal geometry, the interaction between the steel dowel and the concrete does not occur only on the front face in the connector thickness (opposite face to the application of force). According to the authors, there is also the contribution of the opposite upper corner of the steel dowel, presenting effects of concrete pressure and friction on the steel dowel. This phenomenon is evident in the numerical results obtained by the authors for the clothoidal connector, graphically presented through the CPRESS and CSHEAR results from Abaqus.

The same analysis was performed with the numerical models of the experimental tests presented by Caldas et al. [29] to assess the influence of connector geometry and suitability for steel failure analysis models. The analysis consisted of selecting the central nodes in the connector thickness on the sides of all three steel dowels that constitute the connector (Fig. 10). For these nodes, the normal and shear stresses (CPRESS and CSHEAR) acting on the connector at different moments of the analysis were plotted. Along with these stresses, the compressive strength value of the concrete below the connector was also plotted (Fig. 11), calculated according to EN 1994-1-1:2004 [32] (Equation 12), to evaluate the interaction steel-concrete evolution throughout the test. By way of comparison, considering that the example presented is a rectangular profile (X model) for which the concrete confinement effects by the steel tube may be less significant, the average concrete compressive strength value obtained experimentally was also plotted.

$$\boldsymbol{\sigma_{c,Rd}} = \boldsymbol{f_{cm}}\left(\mathbf{1} + \boldsymbol{\eta_{cL}}\frac{\boldsymbol{t}}{\boldsymbol{a}}\frac{\boldsymbol{f_y}}{\boldsymbol{f_{cm}}}\right)\sqrt{\frac{\boldsymbol{A_c}}{\boldsymbol{A_1}}} \;\leq\; \frac{\boldsymbol{A_c f_{cm}}}{\boldsymbol{A_1}}, \;\leq\; \boldsymbol{f_y} \tag{12}$$

where: $\sigma_{c,Rd}$ is the compressive strength of the concrete below the connector in composite columns; f_{cm} is the average concrete compressive strength; η_{cL} is equal to 4.9 for circular sections and 3.5 for square sections; t is the steel tubular profile thickness; a is the diameter or width of the steel tubular profile; f_y is the steel yield strength of the tube; A_c is the concrete cross-sectional area; A_1 is the concrete loaded area under the steel connector.

Fig. 10 shows the identification of steel dowels in the connector. They were numbered from 1 to 3 from the region of force application to the tube during the test (top of the composite column filled with concrete). Fig. 10 shows the connector in its original position, before the start of the test and with its final deformation. The sequence of nodes for which the pressure on the connector was analyzed was taken from the lower curved base to the end of the upper curvature, for all steel dowels, in the front and rear region, as highlighted for dowel 3 in Fig. 10**.**

Differently from the clothoidal connector studied by Kozuch and Lorenc [15], the connector with regular rectangular cutoff does not present concrete pressure effects on the left side, on the thickness of the steel dowel (region marked in blue in Fig. 11), except for the last increment, when small stresses appear in dowel 3, as the concrete is contained by steel dowels 2 and 3. The same happens for the upper left corner of the dowel, which does not present a stress peak as observed for the clothoidal connector. Cardoso et al. [2] highlights that the main failure mode in Crestbond connectors applied in CFST occurs by steel dowel yielding; therefore, the interlocking of the dowel upper left corner has little influence on the other failure modes.

Fig. 11 shows the sequence with the main increments of the X model numerical analysis, presented by Caldas et al. [29]. It shows the distribution of von Mises, CPRESS, CSHEAR stresses and the compressive strength of the concrete below the connector in composite columns according to EN 1994-1-1:2004 [32]. The plotted values correspond only to the right side of the steel dowels, opposite the direction of force application on the CFST, for which there is pressure from the concrete against the connector. The first increment represented corresponds to the beginning of the flow in the dowels lower corners (increment 23). In the next increment (28) a yield stress of 390 MPa is reached in the entire lower section of the third steel dowel. In increment 37 the three steel dowels present yield stresses in the lower sections. The increment 234 corresponds to

the instant when the maximum load is reached in the simulation. The increment 364 corresponds to the end of the simulation. Fig. 12 presents the force *versus* slip curve with the experimental and numerical results for the X model.

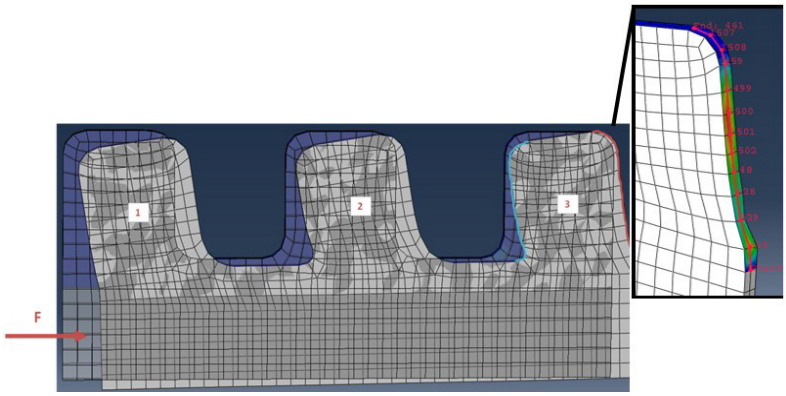

Fig. 10 - Steel dowel identification depending on the load application during the test. Detail of the sequence of nodes in the third dowel.

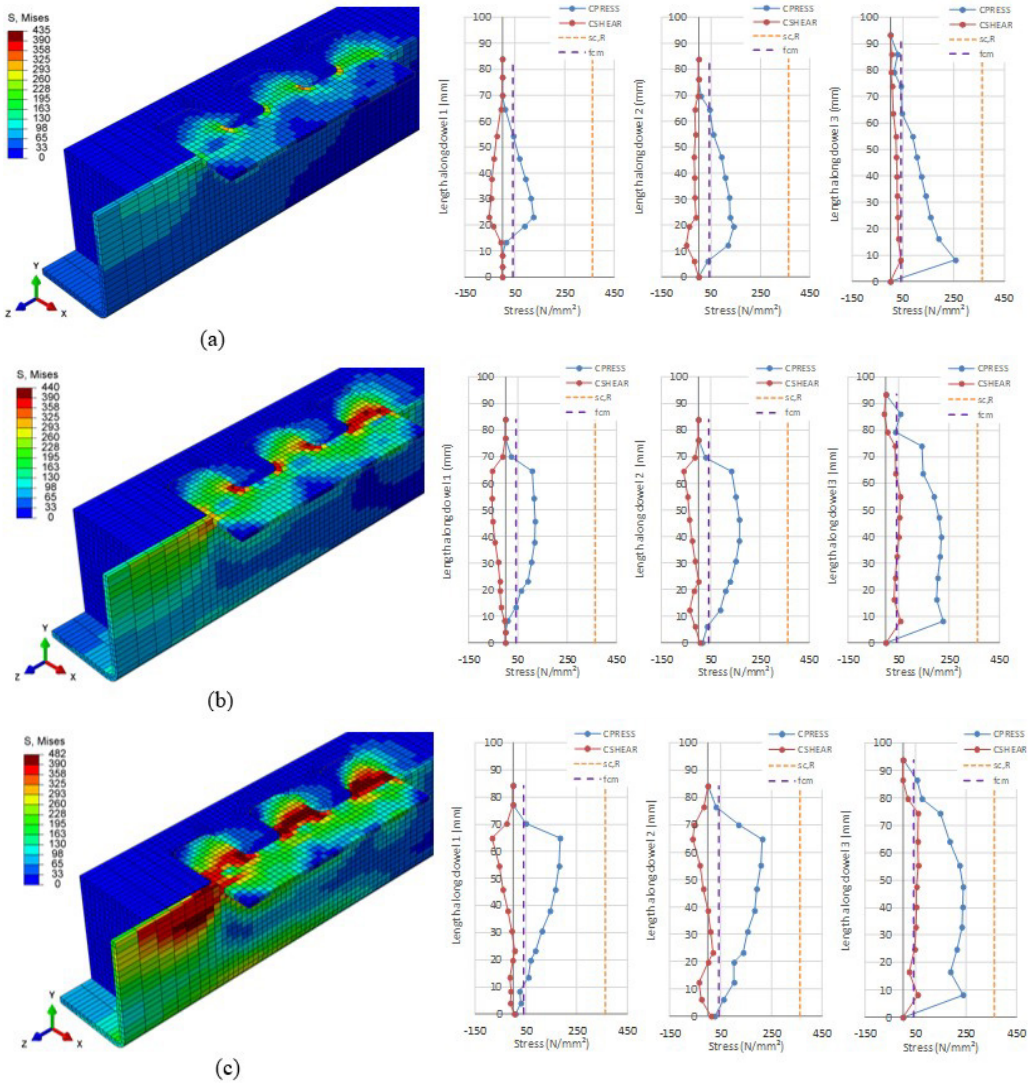

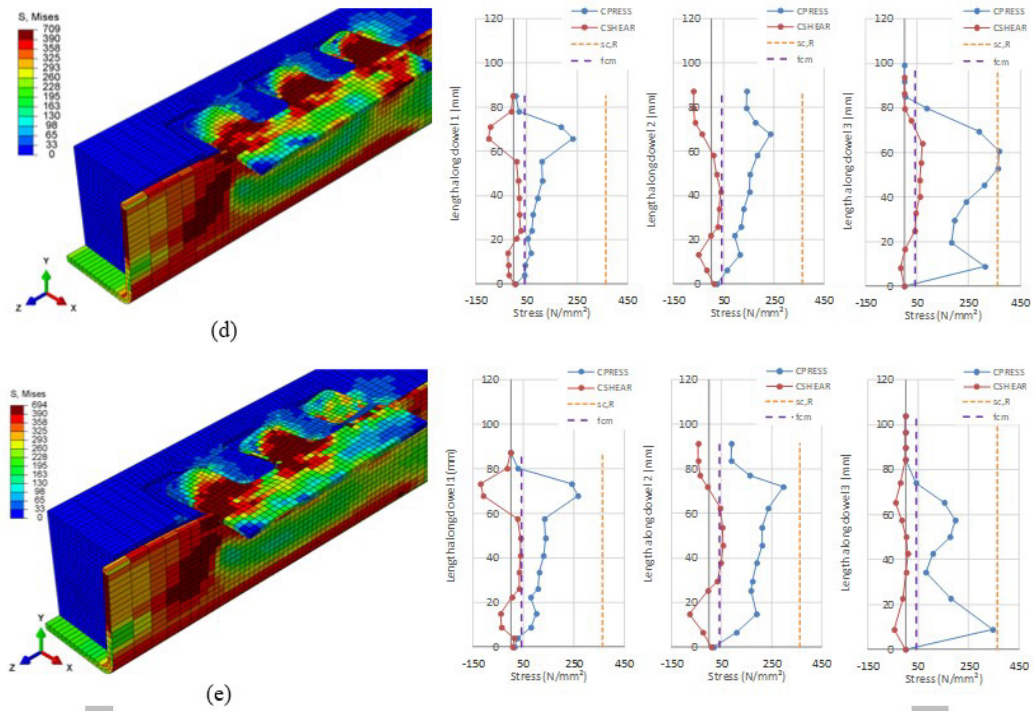

Fig. 11 - Sequence of numerical results for X model, according to Caldas et al. [29]. Von Mises stresses, CPRESS and CSHEAR for: Increment 23 (a), Increment 28 (b), Increment 37 (c), Increment 234 (d) and Increment 364 (e).

From the results found for increment 28, it is possible to observe that the normal stresses distribution is approximately uniform along the steel dowel height, except for the lower and upper curved corners. In this case, the pressure of the concrete on the steel dowel could follow a uniform distribution as suggested by Feldman et al. [31], however, it is worth noting that in this increment only the third steel dowel reached yield stresses in the entire lower section, and the load imposed on the composite system corresponds to 54% of the maximum load achieved in the simulation. As the simulation progresses, all steel dowels show large areas where the 390 MPa stress has been exceeded. In these cases, the pressure distribution changes significantly, no longer resembling a uniform distribution. In increment 234, when the maximum load is reached, the normal stress (CPRESS) in the third dowel reached the value of 363 MPa, corresponding to the compressive strength of the concrete below the connector in composite columns according to EN 1994-1-1:2004 [32].

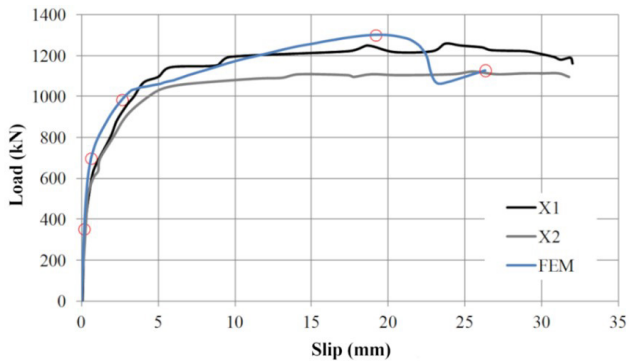

Fig. 12 - Force versus slip curve with experimental and numerical results of the X model, with the corresponding increments represented.

The CPRESS results are given by the program as a normal pressure that is exerted on the deformed connector (effect of the concrete and steel dowel interaction). Therefore, it is necessary to determine the angle with the horizontal (z) and vertical (x) axes at each node for which the result is given. Given the angle it is possible to calculate the

horizontal and vertical components of CPRESS (Fig. 12a, d, g) and CSHEAR (Fig. 12b, e, h). The forces in the horizontal and vertical directions are then calculated by adding up all the vertical and horizontal components (due to CPRESS and CSHEAR).

The resultant pressure and shear force acting on each steel dowel with the approximate centroid position is shown in Fig. 13. The centroid position is calculated from the graph area (Fig. 14c**,** Fig. 14f**,** Fig. 14i), for the deformed connector, in this way it is possible to determine at which height of the steel dowel the resultant force is acting. The resultant force on each dowel is represented in terms of force F, which corresponds to the maximum force applied per dowel according to numerical simulation ($q_{cn,Num}$) for X model. Kożuch and Rowiński [34] and Lechner [16] show in their works images similar to Fig. 13, where the position of the force F and the direction of the cracks in the steel dowels are highlighted for clothoidal connectors. In these connectors, the crack occurs on two opposite sides of the steel dowel and with an inclined direction at the base, which leads the authors to state that the model proposed by Feldman et al. [31] with a straight critical section would not be valid for the connector. On the other hand, for the connector with regular rectangular cutoff, even with the resultant force inclined (similar to that presented by Kożuch and Rowiński [34]) the plasticized region (in the critical section) when the loading reaches its maximum value in the numerical analysis is approximately rectilinear next to the base of all steel dowels.

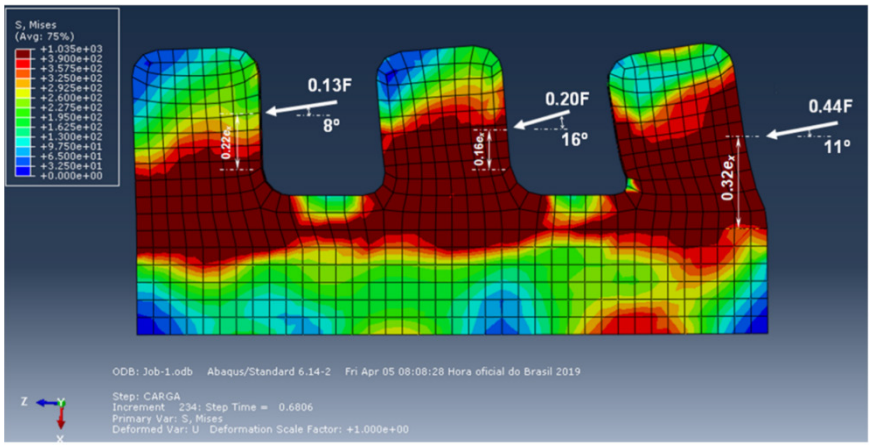

Fig. 13 - Connector behavior mechanical model from numerical analysis.

It is also observed that the forces distribution between steel dowels is not linear (0.13F in the first dowel, 0.20F in the second and 0.44F in the third). The sum of the forces acting on the steel dowels results in 0.77F, which suggests that part of the applied force may be resisted by the steel tube, due to the restriction on the connector output.

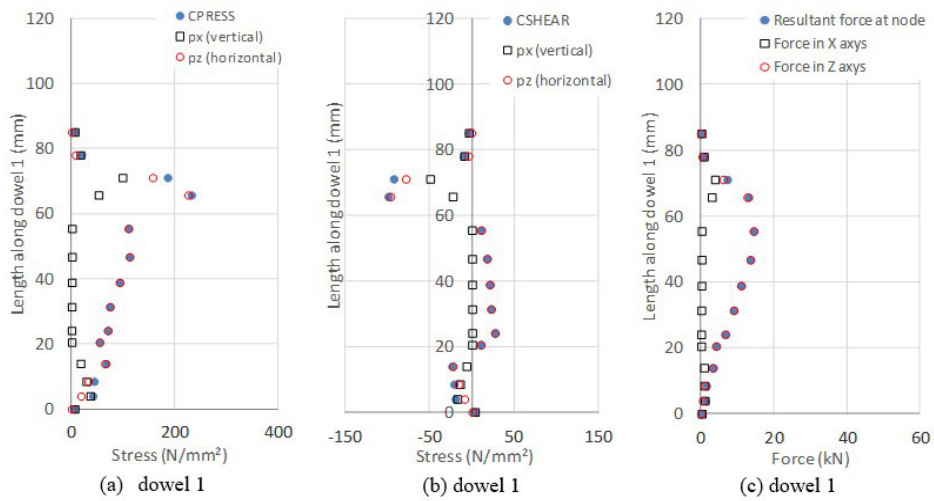

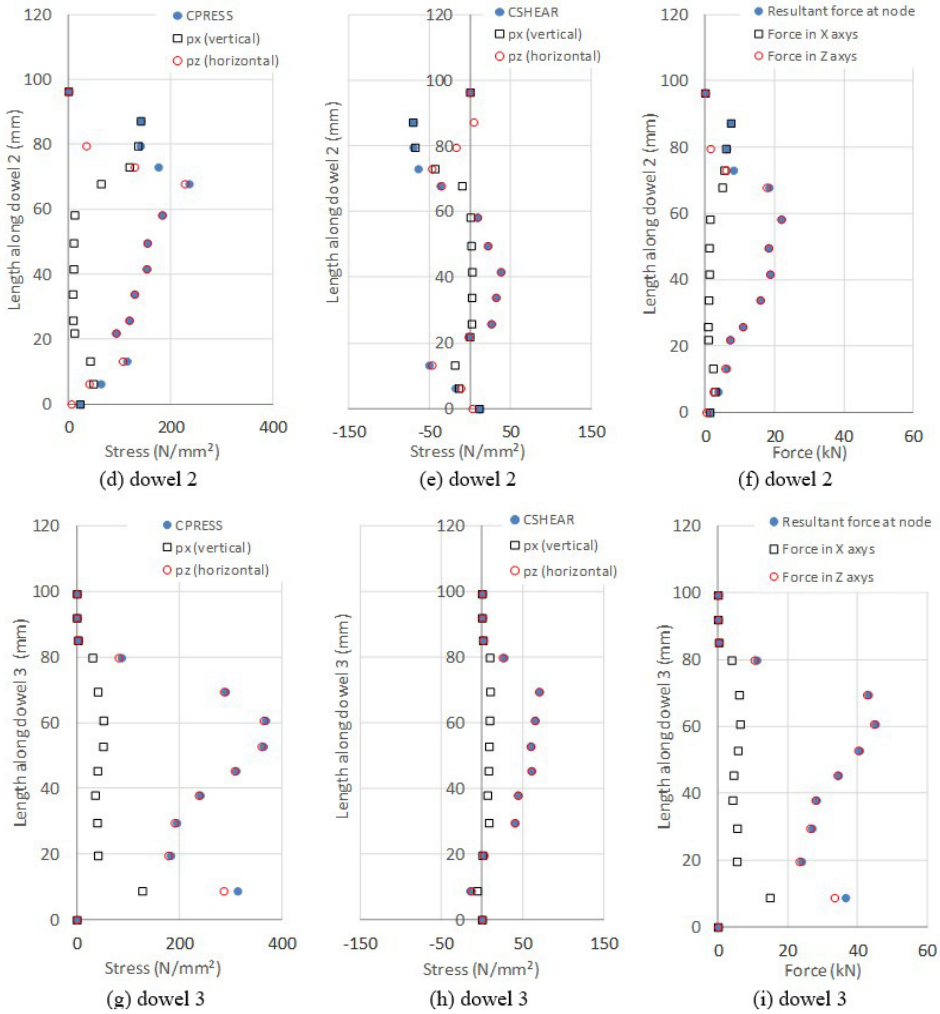

Fig. 14 - Normal pressure distribution on the connector (a, d, g), friction distribution in the connector (b, e, h) and resulting force on the connector side (c, f, i).

4 CONCLUSION

In this work, the deduction of the steel failure equation for the connector with regular rectangular cutoff was presented, according to the von Mises criterion. The results produced with the equation were compared with experimental results found in the literature and with numerical results produced within the scope of this work. A study on the connector shape coefficient was also presented, comparing values obtained for the connector with regular rectangular cutoff with other geometries.

It was observed that the understanding of the shape coefficient varies among different authors in the literature, considering the smaller steel dowel width as a critical section or calculating the position of the critical section in the steel dowel in an iterative process. The equation deduced for the steel failure according to the von Mises criterion for the connector with regular rectangular cutoff led to the most conservative shape coefficient of all the analyzes (54% of the experimental average shape coefficient), but identical to that adopted by the document Z-26-4.56 [14] for clothoidal and puzzle geometries.

The results of numerical simulations were used to study the stress distribution on the connector steel dowels. Consideration of the stress distribution as uniformly distributed along the steel dowel height (except for the curved upper corner) as suggested by Feldman et al. [31] for the steel failure strength equation deduction is valid only for the beginning of the loading process, when only the third dowel presents yielding of the entire section. In the increment corresponding to the maximum loading, the three steel dowels show yielding throughout the section, and the distribution of normal stresses in all is quite different from a uniform distribution (stresses are greatest near the top of the steel dowel).

Furthermore, in the third steel dowel, the compressive strength value of the concrete below the connector in composite columns ($\sigma_{c,Rd}$) is reached.

ACKNOWLEDGMENT

This work was funded by Brazilian research agencies CAPES, CNPq and FAPEMIG. The authors are also grateful for the support provided by IFSULDEMINAS.

REFERENCES

[1] F. Leonhardt, W. Andrä, H. P. Andrä, and W. Harre, "Neues vorteilhaftes verbundmittel für stahlverbund-tragwerk mit höher dauerfestigkeit," *Beton Stahlbetonbau*, vol. 82, no. 12, pp. 325–331, 1987.

[2] H. S. Cardoso, O. P. Aguiar, R. B. Caldas, and R. H. Fakury, "Composite dowels as load introduction devices in concrete-filled steel tubular columns," *Eng. Struct.*, vol. 219, pp. 110805, 2020.

[3] M. Kopp et al., "Composite dowels as shear connectors for composite beams – background to the design concept for static loading," *J. Construct. Steel Res.*, vol. 147, pp. 488–503, 2018.

[4] D. Kraus and O. Wurzer, "Nonlinear finite element analysis of concrete dowels," *Comput. Struc.*, vol. 64, no. 5/6, pp. 1271–1279, 1997.

[5] S. Heinemeyer, "Zum Trag- und Verformungsverhalten von Verbundträgern aus ultrahochfestem Beton mit Verbundleisten," PhD dissertation, Rheinisch-Westfälischen Technischen Hochschule, Aachen, 2011.

[6] R. L. J. Almeida, G. S. Veríssimo, J. C. L. Ribeiro, J. L. R. Paes, M. C. Petrauski, and R. B. Caldas, "Capacidade Resistente do conector Crestbond à falha do aço desencadeada por um mecanismo combinado de cisalhamento e flexão," *Rev. Estrutura Aco*, vol. 9, no. 1, pp. 61–80, 2020.

[7] C. Zapfe, "Trag- und Verformungsverhalten von Verbundträgern mit Betondübeln zur Übertragung der Längsschubkräfte," PhD dissertation, Institut für Konstruktiven Ingenieurbau, Universität der Bundeswehr, München, 2001.

[8] A. R. Alves, I. B. Valente, W. B. Vieira, and G. S. Veríssimo, "Prospective study on the behavior of composite beams with an indented shear connector," *J. Construct. Steel Res.*, vol. 148, pp. 508–524, 2018.

[9] A. R. L. Alves, M. I. B. Valente, W. B. Vieira, and G. S. Veríssimo, "Estudo experimental e numérico sobre o comportamento de vigas mistas com conector Crestbond," in *X Congresso de Estruturas Metálicas e Mistas*, Coimbra, Portugal, 2015.

[10] G. S. Veríssimo, "Desenvolvimento de um conector de cisalhamento em chapa dentada para estruturas mistas de aço e concreto e estudo do seu comportamento," PhD dissertation, Engenharia de Estruturas, Escola de Engenharia, Universidade Federal de Minas Gerais, Belo Horizonte, 2007.

[11] G. S. Veríssimo, I. Valente, J. L. R. Paes, P. J. S. Cruz, and R. H. Fakury, "Concepção e avaliação do desempenho de um novo conector de cisalhamento para estruturas mistas de aço e betão," in *VI Congresso de Construção Metálica e Mista*, Porto, 2007, pp. II-569-II-578.

[12] G. Seidl et al., *Prefabricated enduring composite beams based on innovative shear transmission (Preco-Beam)*, Brussels: Publications Office of the European Union, 2013.

[13] G. Seidl et al., *Prefabricated enduring composite beams based on innovative shear transmission (Preco+)*, Brussels: Publications Office of the European Union, 2013.

[14] Deutsches Institut für Bautechnik, *Allgemeine bauaufsichtliche Zulassung der Verbunddübelleiste*, No. Z-26.4-56, 2018.

[15] M. Kozuch and W. Lorenc, "The behaviour of clothoid-shaped composite dowels: Experimental and numerical investigations," *J. Construct. Steel Res.*, vol. 167, pp. 105962, 2020.

[16] T. Lechner, "Zur Anwendung von Verbunddubelleisten in schlanken Verbundtragern aus ultrahochfestem Beton", " PhD dissertation, Technische Universitat Munchen, München, 2017.

[17] W. Lorenc, "Non-linear behaviour of steel dowels in shear connections with composite dowels: design models and approach using finite elements," *Steel Constr.*, vol. 9, no. 2, pp. 98–106, 2016.

[18] W. Lorenc, M. Kożuch, and S. Rowiński, "The behaviour of puzzle-shaped composite dowels. Part II: Theoretical investigations," *J. Construct. Steel Res.*, vol. 101, pp. 500–518, 2014.

[19] W. Lorenc, "Composite dowels: the way to the new forms of steel - concrete composite structures," in *IABSE Symposium*, Wroclaw Poland, 2020

[20] W. Lorenc, M. Kożuch, and S. Rowiński, "The Behaviour of puzzle-shaped composite dowels - part i: experimental study," *J. Construct. Steel Res.*, vol. 101, pp. 482–499, 2014.

[21] Forschungsvereinigung Stahlanwendung e. V., *P 1208 Consistent design model for production-optimized composite dowels - Basis for DASt guideline and transfer to Eurocode 4*, Düsseldorf: FOSTA, 2021.

[22] H. S. Cardoso, "Avaliação do comportamento de conectores constituídos por chapas de aço com recortes regulares - ênfase em conectores de geometria Crestbond aplicados em pilares mistos," PhD dissertation, Universidade Federal de Minas Gerais, Belo Horizonte, 2018.

[23] L. R. Santos, H. S. Cardoso, R. B. Caldas, and L. F. Grilo, "Finite element model for bolted shear connectors in concrete-filled steel tubular columns," *Eng. Struct.*, vol. 203, pp. 109863, 2020.

[24] L. R. Santos, R. B. Caldas, L. F. Grilo, H. Carvalho, and R. H. Fakury, "Design procedure to bearing concrete failure in concrete-filled steel tube columns with bolted shear connectors," *Eng. Struct.*, vol. 232, pp. 111910, 2021.

[25] L. R. Santos, R. B. Caldas, J. A. Prates, F. C. Rodrigues, and H. S. Cardoso, "Design procedure to bearing concrete failure in composite cold-formed steel columns with riveted bolt shear connectors," *Eng. Struct.*, vol. 256, pp. 114003, 2022.

[26] O. P. Aguiar, "Estudo do comportamento de conectores Crestbond em pilares mistos tubulares preenchidos com concreto," PhD dissertation, Escola de Engenharia, Universidade Federal de Minas Gerais, Belo Horizonte, 2015.

[27] E. G. Silveira "Estudo do comportamento de conectores em chapa com recortes regulares retangulares aplicados em pilares mistos preenchidos com concreto," PhD dissertation, Universidade Federal de Minas Gerais. Belo Horizonte. 2019.

[28] A. C. Pereira, "Estudo numérico dos conectores Crestbond em pilares mistos esbeltos," M.S. thesis, Universidade Federal de Minas Gerais, Belo Horizonte, 2020.

[29] B. Caldas, R. H. Fakury, G. S. Veríssimo, F. C. Rodrigues, and H. C. Cardoso, "Análise experimental de transferência de esforços entre os componentes de aço e concreto de pilares mistos tubulares preenchidos utilizando conectores formados por chapas com dentes retangulares", Relatório final de pesquisa, Edital FAPEMIG 01/2015, Demanda Universal APQ-01117-15, Belo Horizonte, 2019.

[30] J. Berthellemy, W. Lorenc, M. Mensinger, S. Rauscher, and G. Seidl, "Zum Tragverhalten von Verbunddübeln–Teil 1: Tragverhalten unter statischer Belastung," *Stahlbau*, vol. 80, no. 3, pp. 172–184, 2011.

[31] M. Feldmann, M. Kopp, and D. Park, "Composite dowels as shear connectors for composite beams – background to the german technical approval," *Steel Constr.*, vol. 9, no. 2, pp. 80–88, 2016.

[32] European Committee for Standardization, *Eurocode 4: Design of Composite Steel And Concrete Structures, Part 1.1: General Rules And Rules For Buildings*, EN 1994-1-1:2004, 2004.

[33] S. Rowinski, "Fatigue strength of steel dowels in innovative shear connection of steel-concrete composite beam," Ph.D. dissertation, Wroclaw University of Technology, Wrocław, 2012.

[34] M. Kożuch and S. Rowiński, "Elastic behaviour of the steel part of a shear connection with MCL composite dowels," *Steel Constr.*, vol. 9, pp. 107–114, 2016.

[35] M. Pavlović, Z. Marković, M. Veljković, and D. Buđevac, "Bolted shear connectors vs. headed studs behaviour in push-out tests," *J. Construct. Steel Res.*, vol. 88, pp. 134–149, 2013.

[36] S. E. Kim and H. T. Nguyen, "Finite element modeling and analysis of a hybrid steel - PSC beam connection," *Eng. Struct.*, vol. 32, no. 9, 2010.

Author contributions: EGS: writing - original draft, investigation, visualization, validation, formal analysis**.** RBC: supervision, project administration, funding acquisition, writing - review & editing**.** LRS: writing - review & editing.

Editors: Leandro Trautwein, Guilherme Aris Parsekian.